

Polarized and unpolarized proton capture on deuterium

S. E. King, N. R. Roberson, and H. R. Weller

*Physics Department, Duke University, Durham, North Carolina 27706
and Triangle Universities Nuclear Laboratory, Duke Station, Durham, North Carolina 27706*

D. R. Tilley

*North Carolina State University, Raleigh, North Carolina 27607
and Triangle Universities Nuclear Laboratory, Duke Station, Durham, North Carolina 27706
(Received 9 January 1984)*

Angular distributions of cross section were measured for the ${}^2\text{H}(p, \gamma){}^3\text{He}$ reaction at $E_x = 9.83, 10.83, 12.78, 15.47,$ and 16.12 MeV and of analyzing power at $E_x = 10.83$ and 16.12 MeV. The data were fitted by expansions of Legendre and, where appropriate, associated Legendre polynomials. The coefficients of those fits are reported. The data at $E_x = 10.83$ and 16.12 MeV were also analyzed under simplifying assumptions to extract the $s = \frac{1}{2}(E1), s = \frac{1}{2}(E2),$ and $s = \frac{3}{2}(E1)$ transition matrix elements, where s represents the incident channel spin. The results indicate that the data are consistent with a 2(3)% $E2$ and a 3(5)% $s = \frac{3}{2}(E1)$ admixture at $E_x = 10.83(16.12)$ MeV. These results are discussed in light of other recent experiments and calculations.

INTRODUCTION

Measurements of the capture of polarized protons by deuterium have been reported previously¹ in the excitation region of ${}^3\text{He}$ ranging from 8.8 to 10.8 MeV. Those data were analyzed, using the channel spin representation, in terms of $s = \frac{1}{2}(E1)$ and $s = \frac{1}{2}(E2)$ capture amplitudes. That analysis indicated that the $E2$ strength present in the p-d capture reaction was $12 \pm 5\%$ of the total cross section—a result much greater than the theoretical estimates of this strength.²⁻⁴

The present work reports an improved data set as compared with that of Ref. 1, made possible by replacing the solid targets of Ref. 1 with gas targets, using *two* NaI detectors, and using a pulsed beam. These changes reduced backgrounds, increased the counting rate, and allowed measurements at additional energies. Furthermore, since recent work⁵ has shown the importance of the D state in ${}^3\text{He}$ on the observed angular distribution data, the new data were analyzed to allow for this effect by including a $s = \frac{3}{2}(E1)$ term, although this required other simplifying assumptions. As will be seen below, the new data and analysis change the amount of $E2$ strength required to explain the observations. The present paper will report the experimental results of this work in a form which should allow a detailed comparison with future three-body calculations.

EXPERIMENTAL DETAILS

The experimental setup used in obtaining the present data was similar to that of Ref. 1, but with several important differences, as described below.

The detector system consisted of two large NaI detectors, each of which was mounted inside a plastic anticoincidence shield. Additional shielding of Pb, B_4C , and paraffin doped with lithium carbonate was also provided, as shown in Fig. 1. The detectors were located on oppo-

site sides of the beam line.

The target consisted of a gas sample as shown in Fig. 1. The gas-containing chamber was a 16 cm diam thin-walled cell which was filled with high purity ($> 99.99\%$) deuterium gas to a pressure of 83.1 kPa for the data at $E_x = 9.83, 10.83,$ and 16.12 MeV; 41.5 kPa for $E_x = 12.78$

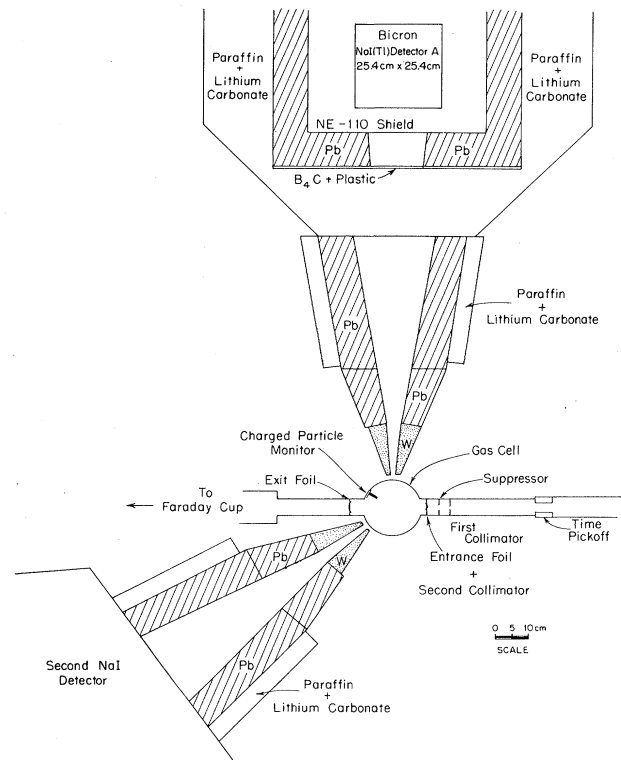


FIG. 1. Experimental setup showing the gas target arrangement, detector collimator assembly, and detector shielding arrangement.

MeV; and 27.7 kPa for $E_x=15.47$ MeV. The entire chamber was lined with tantalum. The entrance foil was a $0.6 \mu\text{m}$ nickel foil, while the exit foil was a $2.5 \mu\text{m}$ Havar foil, the thicker foil here being necessitated by the larger area required for the larger diameter of the outgoing beam. The NaI detectors were collimated to view the central region of the gas by means of tungsten and lead collimating assemblies as shown in Fig. 1. The length of gas viewed at 90° was 1.9 cm. The data were corrected for the change in target thickness as a function of angle by means of a Monte Carlo calculation which took account of the finite geometry of the beam, the collimating assembly, and the NaI detectors. Attenuation effects in the edges of the collimator assembly were also considered. The correction factor was found to be within a few percent of the first order approximation of $\sin\theta$ for angles and energies at which measurements were performed.

The polarized beams used in the present work were produced by the Triangle Universities Nuclear Laboratory (TUNL) Lamb-shift source. Beam polarizations which were measured using the quench-ratio method⁶ were typically 0.62 ± 0.03 . These beams were ramped and bunched⁷ to produce a 2–3 nsec beam burst at a frequency of 4 MHz. The pulsed beam was then used to produce a time-of-flight spectrum which allowed for discrimination against neutron-induced events in the detectors. The time window during which events were accepted was approxi-

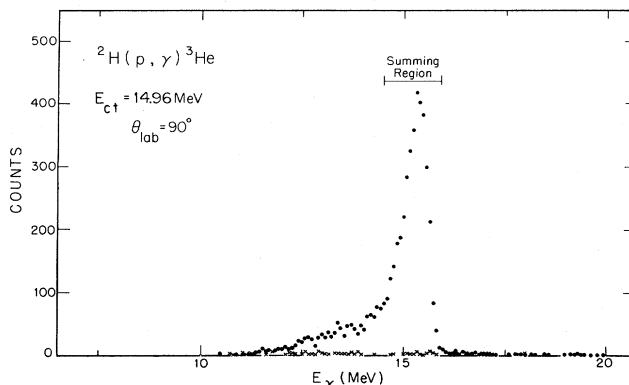


FIG. 2. Spectrum obtained at $E_{ct}=14.96$ MeV and $\theta=90^\circ$ (solid dots). The background spectrum (crosses) obtained by plugging the collimator is also shown. A threshold discriminator was set to reject counts below approximately 10.5 MeV. The summing region (see the text) is noted.

mately 10 nsec. This time requirement also lowered the cosmic-ray count rate thus producing an additional reduction in the background. The reaction was monitored by two silicon surface barrier detectors located at $\theta_{lab}=\pm 25^\circ$. The ${}^2\text{H}(p,p){}^2\text{H}$ reaction yield was used to normalize the data of a given angular distribution.

A typical γ -ray spectrum is shown in Fig. 2 (solid dots)

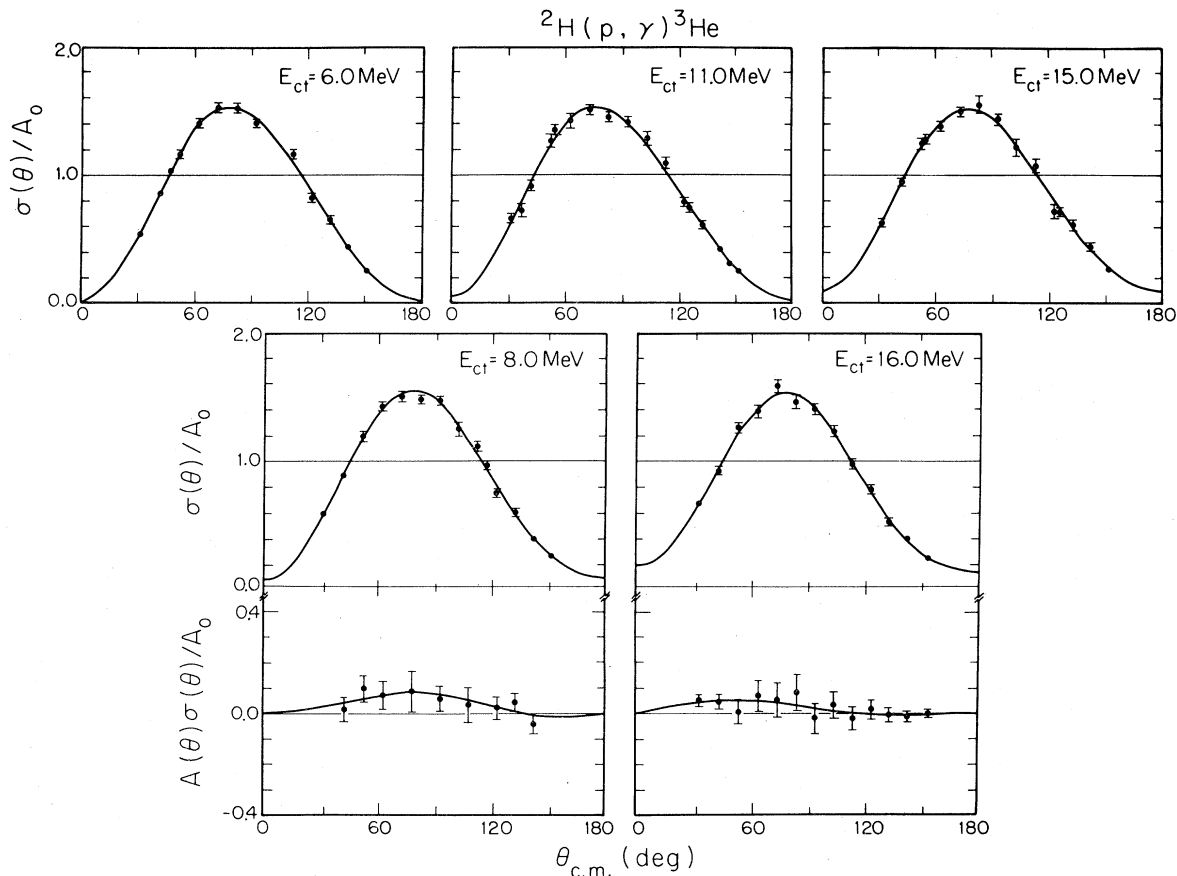


FIG. 3. Angular distributions of cross section and analyzing power for the ${}^2\text{H}(p,\gamma){}^3\text{He}$ reaction. Error bars are statistical errors only. The smooth curves are the result of fits by Legendre and associated Legendre series (see the text). Center of target proton energies (rounded to nearest 0.1 MeV) are noted.

along with a background spectrum (crosses). This background spectrum was obtained by inserting a 15 cm lead plug in the NaI collimating assembly shown in Fig. 1. The background-subtracted spectra were fitted to a standard line shape⁸ to determine a centroid and width in each case. The data were then summed over a region which extended from 1.5 widths below the centroid to 1.1 widths above it. The final sums were corrected for dead time, accidental rejection in the shield, and missed time pickoff signals—a problem which occurred only when the pulsed-polarized beam intensity fell below 60 nA. Typical beam currents were 50–100 nA on target.

Polarized beam measurements were performed at center-of-target beam energies (E_{ct}) of 8.0 and 15.94 MeV, corresponding to E_x of 10.83 and 16.12 MeV, respectively. For the case of $E_{ct}=8.0$ MeV, the pulsed polarized beam had an intensity which was too low to produce reliable timing signals. However, for beam ener-

gies in the region around 8 MeV, high quality spectra could be obtained with a $500 \mu\text{g}/\text{cm}^2$ solid CD_2 target and an unpulsed polarized beam. All other data reported here, including the unpolarized measurements at $E_x=10.83$ MeV, were obtained with the gas target assembly. Spectra were taken with the detectors placed at $\pm\theta$ for spin-up and spin-down beams. The analyzing powers [$A(\theta)$] were then computed from the expressions

$$A(\theta) = \frac{1}{P} \frac{r-1}{r+1}$$

and

$$r^2 = \frac{L_+ R_-}{L_- R_+},$$

where L_+ (L_-) represents the number of counts obtained in the left detector for a spin up (down) beam, R_+ (R_-)

TABLE I. Coefficients and standard deviations from fits of Legendre polynomials to cross section data and associated Legendre polynomials to analyzing-power-times-cross-section data. The χ^2 per degree of freedom obtained for each fit is also given.

E_x (MeV)	E_{ct} (MeV)	Legendre coefficients		χ^2
9.83	6.5	a_1	0.222 ± 0.008	1.47
		a_2	-0.961 ± 0.010	
		a_3	-0.230 ± 0.018	
		a_4	-0.034 ± 0.019	
10.83	8.0	a_1	0.256 ± 0.014	1.78
		a_2	-0.933 ± 0.021	
		a_3	-0.261 ± 0.037	
		a_4	0.017 ± 0.046	
		b_1	0.057 ± 0.022	0.62
		b_2	0.018 ± 0.012	
		b_3	-0.016 ± 0.013	
		b_4	-0.012 ± 0.014	
12.78	10.93	a_1	0.278 ± 0.012	1.23
		a_2	-0.907 ± 0.023	
		a_3	-0.264 ± 0.031	
		a_4	-0.058 ± 0.034	
15.47	14.96	a_1	0.266 ± 0.013	0.98
		a_2	-0.889 ± 0.022	
		a_3	-0.268 ± 0.030	
		a_4	-0.021 ± 0.037	
16.12	15.94	a_1	0.294 ± 0.009	1.16
		a_2	-0.869 ± 0.015	
		a_3	-0.269 ± 0.026	
		a_4	0.040 ± 0.030	
		b_1	0.028 ± 0.012	0.70
		b_2	0.018 ± 0.006	
		b_3	0.003 ± 0.005	
		b_4	-0.001 ± 0.004	
"15"	(combined)	a_1	0.321 ± 0.006	7.1
		a_2	-0.904 ± 0.007	
		a_3	-0.317 ± 0.007	
		a_4	-0.085 ± 0.008	

the same for the right detector, and P represents the beam polarization. The angular distributions of cross section were obtained using unpolarized beams at center-of-target beam energies (E_{ct}) of 6.5, 8.0, 10.93, 14.96, and 15.94 MeV, corresponding to E_x of 9.83, 10.83, 12.78, 15.47, and 16.12 MeV, respectively. The angular distribution data corrected for finite geometry effects and converted to center-of-mass coordinates are shown in Fig. 3.

The solid lines in Fig. 3 are the result of fitting polynomial expansions to the data. In the case of the cross section data the expansion was

$$\sigma(\theta) = A_0 \left[1 + \sum_{k=1}^4 a_k P_k(\cos\theta) \right],$$

while for the product of the cross section and the analyzing power the expansion was

$$\frac{A(\theta)\sigma(\theta)}{A_0} = \sum_{k=1}^4 b_k P_k^1(\cos\theta).$$

These series were terminated at $k=4$ since higher order terms were found to be statistically unjustified. The a_k and b_k coefficients, along with their statistical uncertainties, and the normalized χ^2 values obtained from each fit, are presented in Table I. The result of a fit to a combined data set (labeled "15" in Table I) which included the present $E_x = 15.47$ MeV data, the $E_x = 15.3$ MeV data of Belt *et al.*,⁹ and the $E_x = 14.75$ MeV data of Skopik *et al.*¹⁰ is also given in Table I (see also Ref. 5) for purposes of comparison. In the case of the $E_{ct} = 6.5$ MeV data, the fit was constrained at 0° in order to prevent the cross section at extreme angles from going negative. All other fits, however, were performed without any constraint conditions.

TRANSITION MATRIX ELEMENT ANALYSIS

A model-independent analysis of these data in terms of the amplitudes and phases of the transition matrix elements is not possible. If $E1$, $E2$, and $M1$ radiation is allowed, there will be 16 amplitudes and 15 relative phases, and we would have 31 unknowns with only 9 observables. Even if only $E1$ and $E2$ radiation is assumed, there are still 11 amplitudes and 10 relative phases. For these reasons, the previous analysis¹ assumed only $s = \frac{1}{2}(E1)$ and $s = \frac{1}{2}(E2)$ terms; this gives four amplitudes and three relative phases or seven unknowns, so that a solution could be obtained.

The calculations reported in Ref. 5 have, however,

shown that the $s = \frac{3}{2}(E1)$ strength which arises from the D -state admixture in the ground state of ${}^3\text{He}$ affects the a_2 coefficient. In order to perform an analysis which allowed for this strength, we used the results of Ref. 5 which showed that for a given multipole ($E1$ or $E2$) the two amplitudes having $s = \frac{1}{2}$ but differing in j were essentially equal and that the relative phase between the two amplitudes of different j was near zero degrees. Based on this result, we assumed only one $s = \frac{1}{2}(E1)$ term, one $s = \frac{1}{2}(E2)$ term, and one $s = \frac{3}{2}(E1)$ term so that there are three amplitudes and two relative phases. We denote these amplitudes by ${}^{2s+1}l$ and their phases by $\phi_{(2s+1)l}$, where l and s refer to the orbital angular momentum and channel spin in the incident channel, respectively. Then the equations for the nine observables can be written in terms of the five unknowns as follows:

$$1.0 = 6({}^2p)^2 + 6({}^4p)^2 + 10({}^2d)^2 \quad \text{normalization,}$$

$$a_1 = 20.78^2 p^2 d \cos(\phi_{2d} - \phi_{2p}),$$

$$a_2 = -6.0({}^2p)^2 + 7.14({}^2d)^2 + 2.87({}^4p)^2,$$

$$a_3 = -20.78^2 p^2 d \cos(\phi_{2d} - \phi_{2p}),$$

$$a_4 = -17.14({}^2d)^2,$$

$$b_1 = 6.798^4 p^2 d \sin(\phi_{4p} - \phi_{2d}),$$

$$b_2 = 3.924^2 p^4 p \sin(\phi_{4p} - \phi_{2p}),$$

$$b_3 = 4.524^4 p^2 d \sin(\phi_{4p} - \phi_{2d}),$$

$$b_4 = 0.0.$$

These equations display the fact that *both* the $s = \frac{1}{2}(E2)$ strength and the $s = \frac{3}{2}(E1)$ strength can affect the value of a_2 and cause it to differ from the pure $s = \frac{1}{2}(E1)$ value of $a_2 = -1.0$.

The above equations were fitted directly to the data in the form of $\sigma(\theta)$ and $A(\theta)\sigma(\theta)$ to find the amplitudes and phases and their errors. The results are presented in Table II. Examination of this table reveals that there are two solutions at each energy with the same amplitudes but different relative phases. Furthermore, the χ^2 values indicate excellent fits so that additional degrees of freedom (more amplitudes and phases) cannot be included meaningfully. We also see that the $s = \frac{3}{2}(E1)$ strength accounts for $3 \pm 2\%$ or $5 \pm 3\%$ of the total cross section, while the $E2$ strength is $2 \pm 1\%$ or $3 \pm 2\%$ at 10.83 or 16.12 MeV in ${}^3\text{He}$, respectively. This $E2$ strength is con-

TABLE II. The T -matrix element amplitudes (given as the percentage of the cross section) and their relative phases resulting from fitting the data by an expression written in terms of the $s = \frac{1}{2}(E1)$, $s = \frac{3}{2}(E1)$, and $s = \frac{1}{2}(E2)$ amplitudes and their relative phases.

E_x (MeV)	$\sigma({}^2p)$ (%)	$\sigma({}^4p)$ (%)	$\phi_{4p} - \phi_{2p}$ (deg)	$\sigma({}^2d)$ (%)	$\phi_{2d} - \phi_{2p}$ (deg)	χ^2
10.83	95 ± 3	3 ± 2	8 ± 6	2 ± 1	-26 ± 29	1.0
10.83	95 ± 3	3 ± 2	172 ± 13	2 ± 1	26 ± 20	1.0
16.12	92 ± 2	5 ± 3	7 ± 6	3 ± 2	-2 ± 26	1.0
16.12	92 ± 2	5 ± 3	173 ± 12	3 ± 2	3 ± 26	1.0

siderably smaller than the previously reported¹ $12 \pm 5\%$. It does, in fact, compare favorably with the $< 2\%$ result of Skopik *et al.*¹⁰ and is close to the $0.5\text{--}1\%$ value indicated by the theoretical calculations of Aufleger and Drechsel.² The differences in the $E2$ strength found here compared with that found in Ref. 1 have two origins. First, the inclusion of the $s = \frac{3}{2}(E1)$ strength has a considerable effect. The second reason is based on the observation that if the pure $s = \frac{1}{2}$ analysis of Ref. 1 is performed with the present data, the $E2$ strength rises to about $5 \pm 1\%$ at $E_x = 10.83$ and $8 \pm 1\%$ at $E_x = 15.78$ MeV. The fact that these latter $E2$ strengths are somewhat less than the previously reported values of Ref. 1 must therefore be due to differences in the data. The cleaner spectra, higher statistical accuracy, and more realistic method of analysis of the present work appear to favor the lower $E2$ results presently being reported.

CONCLUSIONS

The use of a gas target arrangement, two NaI spectrometers, and a pulsed polarized beam has provided a substantial improvement in the quality and quantity of the data available on the ${}^2\text{H}(p,\gamma){}^3\text{He}$ reaction for E_p between 6 and 16 MeV. If these data are analyzed assuming one $s = \frac{1}{2}(E1)$, one $s = \frac{1}{2}(E2)$, and one $s = \frac{3}{2}(E1)$ amplitude,

the solutions indicate an $E2$ strength which varies from $(2 \pm 1)\%$ to $(3 \pm 2)\%$ of the total cross section at the energies studied, and an $s = \frac{3}{2}(E1)$ strength which varies from $(3 \pm 2)\%$ to $(5 \pm 3)\%$. This latter strength can arise from the D -state admixture in the ground state of ${}^3\text{He}$. A model calculation⁵ of this strength using Faddeev generated wave functions predicts an $s = \frac{3}{2}$ capture strength of about $0.75\text{--}1.5\%$ at these energies. Our data are in essential agreement with the results of these calculations.

The present value of the $E2$ strength ($2 \pm 1\%$ at 10.83 MeV and $3 \pm 2\%$ at 16.12 MeV) is appealing for two reasons. First, these results are consistent with a recent experiment using the ${}^3\text{He}(e,d)e'p$ reaction which determined that the $E2$ cross section was less than 2% of the total near 15 MeV in ${}^3\text{He}$. And second, theoretical evaluations to date² have predicted an $E2$ strength of the order of 1% (*not* 10%) of the total cross section in this energy region.

It should be noted that while the present T -matrix element analysis provides a possible solution to the anomalous $E2$ strength previously reported in this reaction, the assumptions made in obtaining this result need to be carefully tested. It is hoped that future *full* three-body calculations which include $E2$ and D -state effects, and which can be compared (directly) to the present experimental results (a_k and b_k coefficients), will provide a deeper understanding of these effects.

¹D. M. Skopik, H. R. Weller, N. R. Roberson, and S. Wender, *Phys. Rev. C* **19**, 601 (1979).

²S. Aufleger and D. Drechsel, *Nucl. Phys.* **A364**, 81 (1981).

³I. M. Barbour and A. C. Phillips, *Phys. Rev. C* **1**, 165 (1970).

⁴I. M. Barbour and J. E. Hendry, *Phys. Lett.* **38B**, 151 (1972).

⁵S. E. King, N. R. Roberson, H. R. Weller, and D. R. Tilley, *Phys. Rev. Lett.* **51**, 877 (1983).

⁶T. A. Trainor, T. B. Clegg, and P. W. Lisowski, *Nucl. Phys.* **A220**, 533 (1974).

⁷S. A. Wender, C. E. Floyd, T. B. Clegg, and W. R. Wylie, *Nucl. Instrum. Methods* **174**, 341 (1980).

⁸H. R. Weller and N. R. Roberson, *IEEE Trans. Nucl. Sci.* **NS-28**, 2, 1268 (1981).

⁹B. D. Belt, C. R. Bingham, M. L. Halbert, and A. Van der Woude, *Phys. Rev. Lett.* **24**, 1120 (1971).

¹⁰D. M. Skopik, J. Asai, D. H. Beck, T. P. Dielschneider, R. E. Pywell, and G. A. Retzlaff, *Phys. Rev. C* **28**, 52 (1983).